# Dual-Readout Calorimetry with a Mo-Doped $PbWO_4$ Electromagnetic Section

Silvia Franchino, for the DREAM collaboration

***Abstract*—A first attempt to use an electromagnetic calorimeter prototype made of Mo-doped $PbWO_4$ crystals in view of the possible application of such a detector in dual-readout hybrid calorimetry is described. The detector is made of a matrix of 7 crystals, read out on both sides with photodetectors, equipped with UV and yellow filters each, in order to separate the scintillation and Cherenkov components using their spectral properties. These two components can also be separated using the time structure of the signal. For this purpose the PMTs were read out with Domino Ring Samplers. Data were taken with electron beams of different energies at the H8 beam line at CERN.**

***Index Terms*—Calorimetry, DREAM, Cherenkov, Crystals.**

## I. Introduction

The Dual-REAdout Method (DREAM) is a promising new technique for high-precision measurements of hadronic showers and jets. High-resolution hadron calorimetry is very relevant for a future high-energy linear $e^+e^-$ collider in order to distinguish, for example, the W and Z bosons decay in jets. As resulting from Monte Carlo simulations, a jet energy resolution of about $30\%/\sqrt{E}$ is required for distinguishing W and Z bosons decays in jets. This resolution has been reached by compensating calorimeters as SPACAL and ZEUS. However, compensating calorimeters have some drawbacks. Indeed, compensation requires large integration volume and time, since it relies on neutron detection, and this is often not possible in a real experiment. Moreover, compensating calorimeters have a modest electromagnetic energy resolution because of the small sampling fraction, necessary in order to achieve compensation. In fact, high-resolution electromagnetic and high-resolution hadronic calorimetry are mutually exclusive: good jet resolution implies poor em resolution and viceversa. Furthermore, it is not possible yet to achieve in hadron calorimetry the same level of precision of em calorimeters because of hadron-specific fluctuations, i.e. em shower fraction and invisible energy fluctuations. Indeed the theoretical achievable limit for hadronic calorimeters is $\sigma/E \approx 15\%/\sqrt{E}$ in lead absorber (the limit value depends on the non perfect correlation between the number of neutrons produced and the invisible energy).

The goal of the DREAM project is to develop an hadronic calorimeter with improved performances with respect to the ones built in the past. Since the resolution is determined by fluctuations, eliminating or reducing the effects of the dominant fluctuations is the key to improving it.

S. Franchino belongs to the Department of Teorethical and Nuclear Physics, Pavia University, and the INFN, Pavia, Italy, e-mail: silvia.franchino@pv.infn.it.

Manuscript received November 21, 2011

In non-compensating calorimeters, the hadronic energy resolution is dominated by fluctuations in the electromagnetic fraction ($f_{em}$). In fact a shower developed by hadrons has an electromagnetic ($em$) component, created mostly by the decay in 2 $\gamma$ of neutral pions, and a non electromagnetic ($non-em$) one, that is mostly due to spallation protons produced in nuclear reactions. The electromagnetic component of the shower develops in the same way as those initiated by high-energy electrons or photons, and the calorimeter, if is not compensating, generates a larger signal per unit deposited energy for the electromagnetic shower component than for the non electromagnetic one. The fraction of the initial hadron energy converted into $\pi^o$ varies strongly from event to event, depending on the detailed processes occurring in the early phase of the shower development, $i.e.$ the phase during which production of these particles is energetically possible. Hence the $f_{em}$ has big fluctuations event by event basis. The Dual Readout Method (DREAM) has shown that the effects of these fluctuations can be eliminated by measuring the $f_{em}$ value event by event. This goal is reached by simultaneously measuring different types of signals which provide complementary information about details of the shower development, as explained later.

The dual readout method was first applied to a fiber calorimeter, the DREAM module, in 2003 [1][2] and later, in 2006, it was extended also to homogeneous calorimeters such as $PbWO_4$, BGO and BSO crystals [3], [4] [5] in order to eliminate sampling fluctuations and to increase the amount of Cherenkov photoelectrons [6].

With the fiber calorimeter, the DREAM Collaboration had first studied how to eliminate the main contributions to hadronic energy fluctuations, i.e. the em shower fraction $f_{em}$ (see later) and the invisible energy fluctuations created by nuclear breakup effects[1].

After the excellent results obtained with this detector, which had established the validity of the concept of the dual-readout technique, other effects such as the sampling fluctuations and the signal quantum statistics were approached. In this context, a wide study of crystal calorimeters was carried out, in order to develop an high-performance em calorimeter using the same readout scheme.

In the following the first preliminary results on Mo-doped

[1]Measuring the signal contributions from neutrons event by event is another aim of the DREAM Collaboration [7]. An estimation of the neutron contribution can be obtained by measuring the time structure of the scintillation signals event-by-event. Indeed neutrons appear as a tail with a characteristic decay constant, which depends on the mean free path of neutrons in the calorimeter ($\approx$ 20 ns in the fiber calorimeter). This tail is absent in the Cherenkov signals, which is clearly insensitive to neutrons, and also in the scintillation signals generated by em showers.

$PbWO_4$ crystal matrix will be presented.
In addition, the DREAM Collaboration had studied the performance of an hybrid calorimeter [8], constituted by the fiber calorimeter and by a BGO crystal em section, by applying the dual-readout technique to both detectors. Without using the dual-readout method, the e/h mismatch would spoil the hadronic resolution because the e/h of a crystal calorimeter is typically $\approx 2$. The application of the dual-readout principles in such a calorimeter may work only if one can detect simultaneously scintillation and Cherenkov signals also in the em section. With this hybrid calorimeter an excellent hadronic and electromagnetic energy resolution may thus be reached (see also proceedings of D. Pinci at this conference).

## II. The dual readout method

The first prototype used to prove the feasibility of the dual readout method was a 10 $\lambda_{int}$ fiber module (figure 1), built in the Texas Tech University in 2001, and studied under testbeams at CERN from 2003. It was made by a copper absorber structure, equipped with fibers of two types of active media: scintillating plastic and quartz.

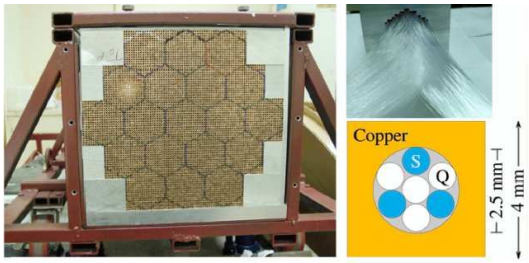


Fig. 1. *Layout of the DREAM fiber calorimeter. The basic element is a 200 cm long extruded copper tube (cross section 4 × 4 $mm^2$, with a central hole of 2.5 mm diameter). Three scintillating fibers (S) and four quartz Cherenkov fibers (C) are inserted in each hole. The calorimeter consists of about 6000 of such tubes. The fibers are split as they exit at the rear into bunches of two types of fibers, and are read with different photomultipliers.*

Hadron showers developing in this detector generate signals in both types of fibers and these signals provide complementary information about the showers. Scintillating plastic fibers produce light for every charged shower particle that crosses them. The amount of scintillation light (S) is, in first approximation, proportional to $dE/dx$: the energy deposited by the shower particles in these fibers. On the other hand, the Cherenkov quartz fibers only produce light (C) when they are traversed by charged particles traveling faster than $c/n$; hence C is created only by the $em$ shower component. In fact, particles of the $non-em$ shower component are usually not sufficiently relativistic to produce Cherenkov light. On the other end, electrons and positrons through which the energy of the $em$ shower component is deposited are relativistic down to a fraction of 1 MeV and thus dominate the production of Cherenkov light in hadron showers [9].
By measuring the signals from both types of fibers simultaneously, one therefore learns how much energy was deposited in the calorimeter and what fraction of that energy was carried by the $em$ shower component. Using the ratio of the two signals (C/S), it is possible to measure, event by event, the value of the electromagnetic fraction $f_{em}$ and the dominant source of fluctuations contributing to the hadronic energy resolution can thus be eliminated. In fact, the hadronic calorimetric response (R), either for the scintillation or the Cherenkov light, can be expressed in terms of $f_{em}$ and the $e/h$ ratio:

$$R(f_{\rm em}) = f_{\rm em} + \frac{1}{e/h}(1 - f_{\rm em}) \quad (1)$$

Defined in this way, R = 1 for $em$ showers. The $e/h$ ratio, $i.e.$ the ratio of the detector response to $em$ and $non-em$ shower components, depends on the choice of the passive and active calorimeter media and on the sampling fraction[2]. Based on Eq. 1, we can write the ratio between the Cherenkov and the scintillation signals as:

$$\frac{C}{S} = \frac{f_{\rm em} + 0.21(1 - f_{\rm em})}{f_{\rm em} + 0.77(1 - f_{\rm em})} \quad (2)$$

where 0.21 and 0.77 represent the $h/e$ ratios of the Cherenkov and scintillator calorimeter structures, respectively. From Eq. 2 it's easy to see that by measuring the C/S ratio, event by event, one can extract the electromagnetic fraction $f_{em}$.

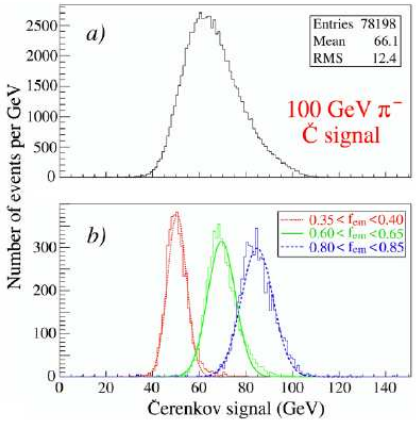


Fig. 2. *Cherenkov signal distribution for 100 GeV $\pi^-$ (a) and distributions for subsamples of events selected on the basis of the measured $f_{em}$ value, using the C/S method (b).*

The merits of this method are clearly illustrated in figure 2, which shows the overall Cherenkov signal distribution for 100 GeV $\pi^-$ (a), as well as distributions for subsamples selected on the basis of their $f_{em}$ value (b), determined by equation (2). Each $f_{em}$ bin probes a certain region of the overall signal distribution, and the average value of the subsample distribution increases with $f_{em}$.
Once the value of $f_{em}$ is determined for a shower, the signals can be corrected in a straightforward way for the effects of non-compensation.
After eliminating the effects of fluctuations in the

[2]This relationship holds separately for both sampling media. The $e/h$ value of a copper/quartz-fiber calorimeter was measured to be $\sim 5$, while for the copper/plastic-scintillator structure is estimated to be 1.4 [10]

electromagnetic energy fraction are eliminated, unfortunately the performance of the hadronic calorimeter is still limited by other fluctuations. In the DREAM detector (see figure 2) these fluctuations include, apart from fluctuations in $side\ leakage$ which can be eliminated by making the detector larger, $sampling\ fluctuation$s and *fluctuations in the Cherenkov light yield*. The latter effect played a prominent role (contributing $35\%/\sqrt{E}$ to the measured resolution) and was caused by the small number of Cherenkov photoelectrons constituting the signals (8 p.e./GeV).
However, there is absolutely no reason why the DREAM principle would only work in fiber calorimeters, or even in sampling calorimeters. One could in principle use a homogeneous (fully sensitive) detector, like dense high-Z crystals (e.g. $PbWO_4$, BGO), whose signals are due to both Cherenkov and scintillations light, provided that the light signals can be separated into scintillation and Cherenkov components. In this way both effects which reduce the resolution of the fiber detector can be eliminated. The challenge is then to extract scintillation and Cherenkov signals from the light generated by showers developing in these crystals. We applied many techniques in order to accomplish this, as explained in the next session.

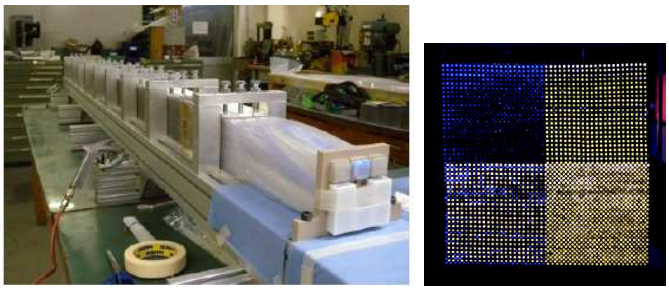

Fig. 3. *(Left) the lead-based newdream prototype built in Pavia and tested at CERN in July and November 2011 , (right) the sampling structure of newdream. The detector will be modular. Each module contains 4 towers, is read out by 8 PMTs. It is 2.5 m long (10 $\lambda_{int}$), has a cross section of 9.6× 9.6 cm$^2$ and a mass of about 150 kg.*

Besides on crystals, the DREAM collaboration is also studying how to improve the sampling fraction and the sampling frequency of the old fiber calorimeter. The design of the New-DREAM prototype is such that fibers are individually embedded in the absorber structure, instead of in groups of seven. in the new detector, the packing fraction of the fibers is roughly doubled, the numerical aperture of the Cherenkov fibers is increased, the upstream end of the Cherenkov fibers is aluminized and the quantum efficiency of the photocathode is increased (using Super Bialkali PMTs). Two prototypes using lead as absorber have already been built and tested recently; one of those is displayed in figure 3. The goal is to build in the next years a full containment calorimeter made of those modules.

## III. The Dual Readout Method with crystals

Since the year 2006, an important part of the DREAM experimental program has concentrated on using high-Z crystals instead of fibers. So far, we have tested $PbWO_4$ (undoped and doped with Molybdenum and Praseodymium), BSO and BGO crystals. [5].
In order to separate the scintillation and Cherenkov components, we have used different characteristics of the two types of light, summarised in Table I.

| | $Cherenkov$ | $Scintillation$ |
|---|---|---|
| Time structure | Prompt | Exponential decay |
| Light spectrum | $1/\lambda^2$ | Peak |
| Directionality | Cone: cos$\theta_C$= $1/\beta$n | Isotropic |
| Polarisation | Polarised | Not polarised |

TABLE I
*Different properties of Cherenkov and scintillation light*

1) Time Structure
   Cherenkov light is prompt, while the scintillation mechanism is characterised by one or several time constants, which determine the pulse shape. High sampling frequency time structure measurements were performed, to study the properties of the prompt component in the signals.
2) Spectral properties
   Cherenkov light exhibits a $1/\lambda^2$ spectrum, while the scintillation spectrum is a specific characteristic of the crystal, because depends on its energetic band structure (Fig 4). Of course, the extent to which these differences may be observed in the measured signals depends also on the filters, if any are used, and on the wavelength dependence of the quantum efficiency of the light detector.
3) Directionality
   Contrary to scintillation light, which is emitted isotropically, Cherenkov light is emitted at a characteristic angle (cos$\theta_C$= $1/\beta$n) by the relativistic (shower) particles that traverse the detector. We measured the signals for different orientations (i.e. angles $\theta$) of the crystal with respect to the beam. Unfortunately this feature, which is very useful for quantitative evaluation of the Cherenkov contribution, cannot be used in a realistic $4\pi$ experiment.
4) Polarisation
   Another difference is that the Cherenkov light is polarised and it is possible to separate it from the scintillation one also by means of polarisation filters [11].

### A. Doping of $PbWO_4$ crystals

In order to use crystals in dual-readout calorimeters, and to have a better separation between the Cherenkov and the scintillation components, a "perfect" crystal should have an emission wavelength far from the bulk of Cherenkov radiation, a scintillation decay time of tenths of nanoseconds, and it shouldn't be too much bright, otherwise the Cherenkov photoelectrons are hidden by the scintillation ones.
Many studies were done in past years about $PbWO_4$ crystals with the goal of an "ideal" crystal for the ECal of the CMS experiment [12], [13], [14]. Some doping elements, if added to the $PbWO_4$ crystals, can achieve a shift of the scintillation spectrum to longer wavelengths, and a longer decay time, as

needed for the Dual Readout.
With no doping, in fact, lead-tungstate crystals show some disadvantages for the dual readout method. The scintillation light is predominantly blue and thus separating it from the Cherenkov one by means of optical filters is not optimal since their spectral region are too close. Moreover the decay of the $PbWO_4$ scintillation light is very fast ($\tau < 10$ns) and it is thus hard to distinguish it from the prompt Cherenkov light by exploiting the different time structure. Both problems can be solved by doping lead-tungstate crystals with small percentages of impurities.
The DREAM Collaboration tested first $PbWO_4$ doped with praseodymium (Pr), with three concentration levels (0.5%, 1%, 1.5%) [15].The scintillation process was unacceptably slow (scintillation components in the $\mu$s range) and made this dopant not suitable for dual-readout calorimetry.
Then, $PbWO_4$ crystals with different Molybdenum (Mo) concentration levels (0.1%, 0,2%, 0.3%, 1%, 5%) have been tested and they resulted to be promising [15], [16].

### *B. Mo-doped $PbWO_4$ crystals*

As we can see from the figure 4, for each Mo-doping concentration the emission spectrum is red-shifted. This is very convenient for the dual-readout purpose. In fact it gives the possibility to use different filters to separate the low-wavelength Cherenkov component from the scintillation one. We have used a short-pass filter (ultraviolet) to detect the Cherenkov light, whereas on the other side of the crystals the PMTs were equipped with a long-pass (yellow) filter.
The strength, the purity and the attenuation of the Cherenkov

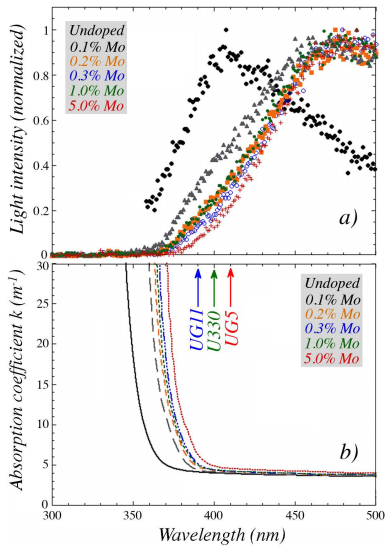


Fig. 4. *Emission (top) and absorption (bottom) spectra, as a function of wavelength, of $PbWO_4$ crystal doped with different concentrations of molybdenum. UG11, U330 and UG5 are three different UV filters used for our tests; arrows in the figure indicate the end of their transmission windows.*

light resulted to depend on the narrow bandwidth between the self-absorption edge and the cutoff of the transmission filter (figure 4 bottom). This dependence is particularly true for the light attenuation. In particular a measurement of the attenuation of the two light components showed that the scintillation was almost independent on the impact point of the shower with respect to the photodetector, while the signals on the UV-filter side decreased with the distance, indicating an absorption of Cherenkov light. This effect is very important for the dual readout and we have tried to limit it; as can be seen from figure 4 bottom, the gap between the self-absorption of the crystal and the UV filter depends both on the filter and on the doping percentage. For each crystal we tested, we have done dedicated measurements of attenuation of Cherenkov light and separability from the scintillation one, by means of spectral property and time structure [16]. High concentrations of molybdenum gave the worst results in almost any respects while 0.1%-1% concentrations seemed to be suitable for dual-readout technique purposes. In particular lead-tungstate crystals doped with 0.3% Mo have revealed optimal, both for spectral separation and temporal response. Among the tested filters (see figure 4 bottom; arrows show the end of the transmission of each filter) we have seen that the U330 one seems so give better results because with the UG11 the transmission window is too narrow and, with the UG5 the signals resulted to be contaminated by short wavelength scintillation light. In figure 11 the Cherenkov signal as a function of the impact point of the shower is displayed for 0.3% Mo-doped $PbWO_4$crystals with the three tested filters. A position scan, in which a 50 GeV electron beam was moved in steps of 2 cm along the longitudinal axis of the crystal, doped with 0.3% Mo, showed that the increased bandwidth offered by the UG5 and U330 filters greatly alleviated the attenuation of Cherenkov light problem. Whereas the crystal response dropped by about a factor of two over 10 cm in the case of the UG11 filter, the decrease was of 10% when a U330 or UG5 filter was used to detect the Cherenkov light.

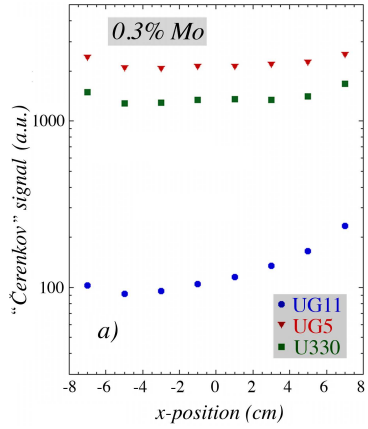


Fig. 5. *Attenuation measurement as a function of UV filter cutoff for a single crystal of $PbWO_4$doped 0.3% with Mo..*

## IV. Mo-doped $PbWO_4$ crystal matrix

After the tests performed on different concentrations of Mo-doping in $PbWO_4$ crystals, we developed and started to test the performances of a 0.3% Mo-doped $PbWO_4$ matrix as an electromagnetic section of a dual readout calorimeter. This is still a preliminary phase in which we tested its performances

only under electron beams. Once the newdream fibre full containment calorimeter will be ready we will test the crystal matrix (or a bigger one) in conjunction with the hadronic section, in order to make an hybrid dual readout calorimeter.

### A. Test beam setup

The matrix was tested at the end of 2010 and in July 2011 at the H8 SPS test line at CERN with electron beams of different energies. The effects of different doping concentration in $PbWO_4$ crystals, shown before, were studied in 2008 and 2009 at the H4 line of the SPS.
The data analysis for 2010 data turned out to be very difficult due to the poor conditions of the electron beam (fundamental for the calibration procedure), while in 2011 many beam monitor detectors were installed, as can be seen in figure 6.
The beam profile could be reconstructed, with a precision of about 200 $\mu$m, by two Delay Wire Chambers (DWC) which were installed upstream and downstream of the trigger counters (in 2010 only one of those was installed)[3]. The timing information of all these tracking chambers was recorded with a 12 bit, 32 channels, CAEN V775 TDC, with a resolution of 0.2472 ns.

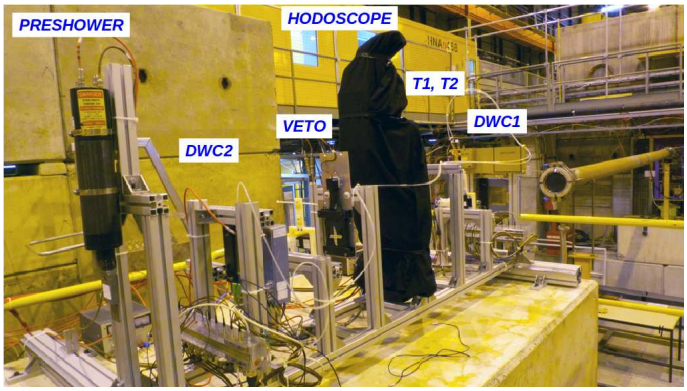


Fig. 6. *Picture taken in November 2011 showing the DREAM test beam setup, and in particular beam detectors that have been installed in the H8 beam line in order to clean up the electron beam.*

Two scintillators with an overlapping region of $4\times4$ cm$^2$ were used as trigger system (T1, T2), and in 2011 the trigger logic was improved using the coincidence between the two scintillators and a "veto" counter that has an hole in the centre with a diameter of 2 cm. Only particles passing through the hole were selected by the trigger; in this way beam halo effects were limited.
In order to remove contaminating pions and muons from the electron beams, we used a preshower detector consisting of a 5 mm thick lead plate followed by a scintillation counter. About 25 m downstream of the experimental setup, after the beam dump (about 20 interaction lengths), a scintillator paddle was used as a muon counter.
The trigger logic was implemented through NIM modules and the signals sent to a VME I/O register, which was also catching the spill and the global busy information. From the testbeam performed in July 2011, the trigger logic was implemented on an FPGA starter kit.
The VME crate was linked to a data acquisition computer through an SBS 617 optical VME-PCI interface that allows memory mapping of the VME resources via an open source driver.
The data acquisition was built around a single-event polling mechanism and performed by a readout program that was streaming physics events and on-spill pedestal events into two independent first-in-first-out buffers. Our readout scheme optimised the CPU utilization and increased the data taking efficiency thanks to the bunch structure of the SPS cycle, where beam particles were provided to our experiment during a spill of 9.6 s, with a repetition period of 48 s.
15 mm thick low-loss cables were used to transport the crystal signals to the counting room (20 m far away) in order to limit distortion of the signal time structure. Faster and shorter cables were used for trigger counters, which generated the gate and trigger the data acquisition.
The matrix was made of 7 crystals $3\times3\times20$ cm$^3$ (Fig 7).

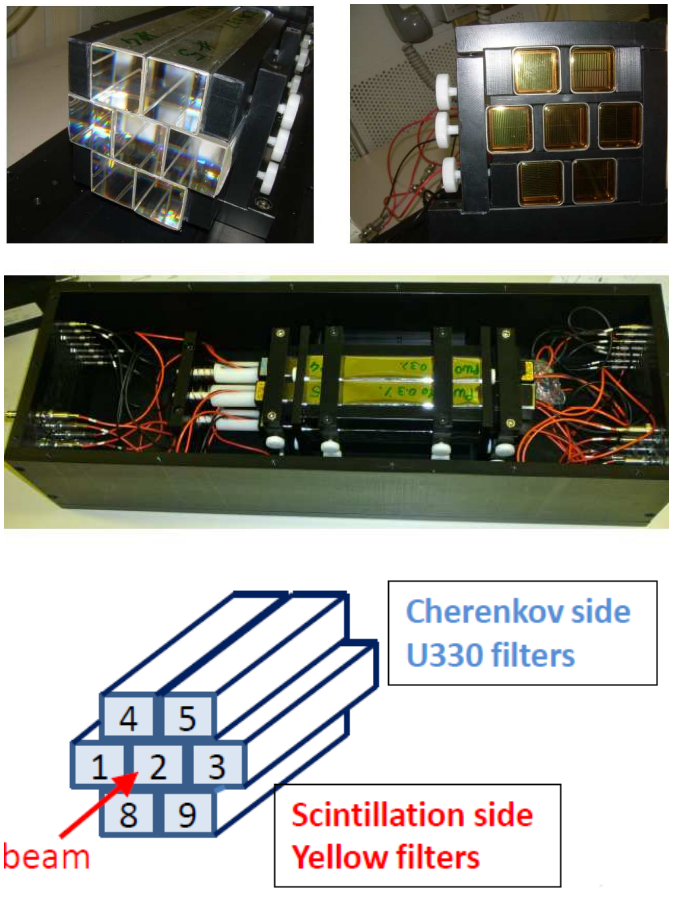


Fig. 7. *Top: pictures of the $PbWO_4$ matrix and its PMTs. Bottom: sketch of the orientation of the matrix with respect to the beam and its filter position.*

Crystals were produced by the Radiation Instruments & New Components company in Minsk (Belarus).
Each crystal was wrapped with mylar in order to avoid photon contamination from outside and to contain photons produced inside the crystal.

[3]In addition to this beam chambers, two fiber hodoscope were also built and installed but they are still under commissioning.

In 2010 testbeam, to extract scintillation light, a yellow filter (Schott GG495) was used. It transmits only light with wavelength longer than the cutoff value (495 nm). For the Cherenkov light an UV filter (Hoya U330) was chosen, as described before.
Each of the used filter was 3 mm thick and made of glass; they were coupled to the crystal and to the PMT by means of elastocil (silicone) "cookies" (n=1.4), which reduced the light trapping effect caused by the large refractive index of lead-tungstate (n=2.1).
Each crystal in the matrix was readout at both sides with PMTs. The 14 PMTS used (Hamamatsu 8900) had a photo-cathode area size of 23.5 $mm^2$, 10 multiplication stages and were equipped with a borosilicate window; for the one detecting Cherenkov light we used the model 8900-100 that has also a superbialkali cathode, in order to increase the quantum efficiency.
In 2011 testbeam, in order to correct effects due to attenuation of Cherenkov light, we tested the configuration in which UV filters were mounted on both ends of the matrix; in this way it was possible to add Cherenkov signals belonging from both upstream and downstream PMTs. Unfortunately this configuration did not allow to extract the scintillation signal with sufficient resolution, in spite of the different time structure of the two signals.
In November 2011 we have then tested another configuration with an UG5 filter on one side and the U330 on the other one. The idea was to extract the scintillation from the tail of light passing through the UG5 one, that has a bigger bandwidth, and hence a contamination with scintillation light. Scintillation signal is extracted using the time information, and integrating the time structure over the tail of the distribution. The Cherenkov light is extracted, and corrected for effects of attenuation, from both upstream and downstream filters. Data with this configuration have still to be analyzed.
The crystal matrix is positioned with the crystal long axis parallel to the beam line. Moreover UV filter is positioned downstream while yellow filter upstream. In this way the matrix is about 22 $X_0$ long.
The time structure of each signal was sampled with the CAEN V1742 board based on the Domino Ring Sampler (DRS) chip that allows time structure measurements of each signal with a sampling rate of 2.5 GHz (0.4 ns time resolution). This module has 32 channels, each of which allows time structure measurements with a resolution that was until now only achievable with digital sampling oscilloscopes [17].

### B. Calibration

The calibration procedure of the 7 crystals was performed by steering 80 GeV electrons in the center of each crystal longitudinally. This was easily feasible since the crystal matrix was mounted on a platform which could move vertically and horizontally. For each crystal, 25000 events were recorded. In addiction, 2500 randomly triggered events provided the pedestal information.
Events were selected after applying cuts on DWC chambers (and PS detector for 2011 data) and a beam spot region of 10 $mm^2$ was selected.
In this geometry, 80 GeV electrons deposited, on average, 66 MeV in the central $PbWO_4$ crystal and 74 MeV in the full matrix, as determined with GEANT-4 MonteCarlo simulations. Lateral leakage, for em showers is negligible, and the longitudinal one estimated to be at the level of 8%.

### C. Results

In figure 8 the average time structure both from the yellow filtered signals and the UV filtered ones are displayed. The solid (blue) line represents the time structure measured on one side of the crystal, where the U330 filter was mounted. The dotted (red) line represents the time structure measured on the other side of the crystal, where the light was filtered by the yellow filter. These two time structures, which were measured for the same sample of events, are spectacularly different. The UV light produced signals that were very fast, $> 90\%$ of the integrated signal was contained in a time interval of only 7 ns. The yellow light produced a signal with a rise time of 5 ns, and this signal decayed to 10% of its maximum value in 64 ns. These characteristics strongly indicate that the light passing the UV filter produced an almost pure Cherenkov signal, while the light passing the yellow filter generated a signal that had all the characteristics of a scintillation signal.

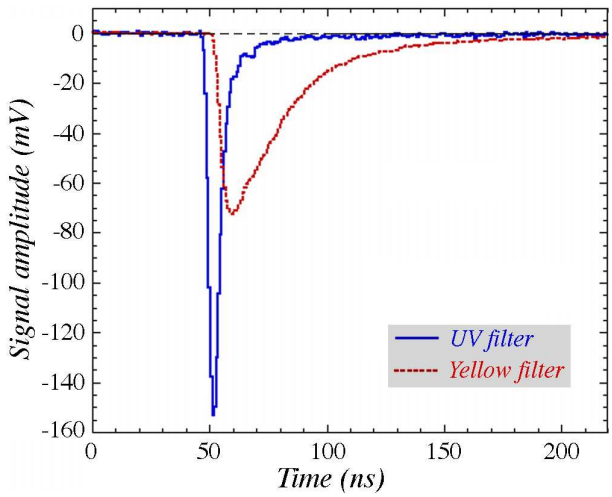


Fig. 8. *Time distributions for UV filtered signals (blue line) and yellow filtered one (red line). The UV signals show a typical Cherenkov time structure, while the yellow one it's scintillation.*

In figure 9 both scintillation and Cherenkov signal distributions for 100 GeV electron beam are displayed. Scintillation signal is taken as the integral, over the full time windows of the yellow-filtered light. The Cherenkov light is the integral over a window of 50 ns around the peak of the UV filtered light. The two distributions are extracted from the 2010 testbeam data, in which no good beam monitor systems were installed. In fact, as is better visible in the scintillation distribution, the response is not a perfect gaussian distribution but it has some events with lower energy deposit; this may come from pion contamination of the electron beam and from longitudinal

leakage effects. The $\sigma/\mu$ value from the gaussian fit for scintillation is about 1.3% and for Cherenkov is 5%.

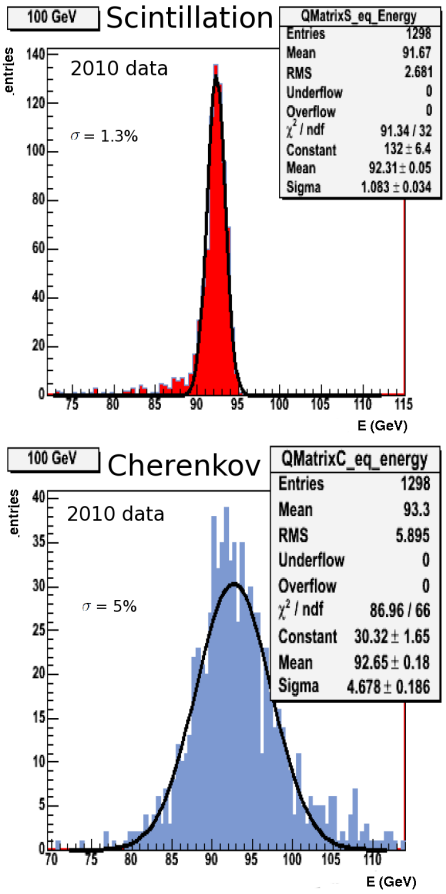


Fig. 9. *Signal distributions for 100 GeV electron beam from 2010 test beam data: Top scintillation from yellow filtered signals, Bottom Cherenkov obtained from U330 filtered signals.*

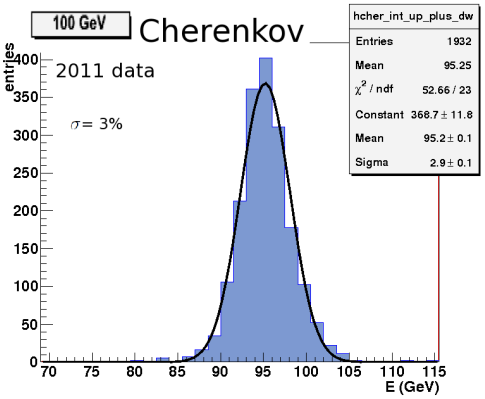


Fig. 10. *Cherenkov distribution for 100 GeV electrons obtained with 2011 data; the sum of upstream and downstream U330 filtered signals was used.*

If figure 10 the Cherenkov distribution, as measured from data taken in the 2011 testbeam, is shown. As explained before, on those data better cuts on both DWC chambers were applied, in conjunction with muon and preshower detectors, in order to select events generated only by electrons. It is possible to see that the energy deposit is well fitted with a gaussian. Furthermore, signals from the upstream and downstream UV filters were added; in this way a better resolution was found because fluctuations coming from the depth of the shower were eliminated. The $\sigma/\mu$ value is then improved from 5% to 3%.

The C/S event by event distribution was also studied for 2010 data; it is gaussian with mean value at one, as expected by em showers, and the $\sigma/\mu$ value is of the order of 4%. This can be improved with the analysis of November 2011 data with a better beam and corrections for Cherenkov self absorption.

In figure 11 the electromagnetic energy resolution measured with the matrix, both for scintillation and Cherenkov light are shown.

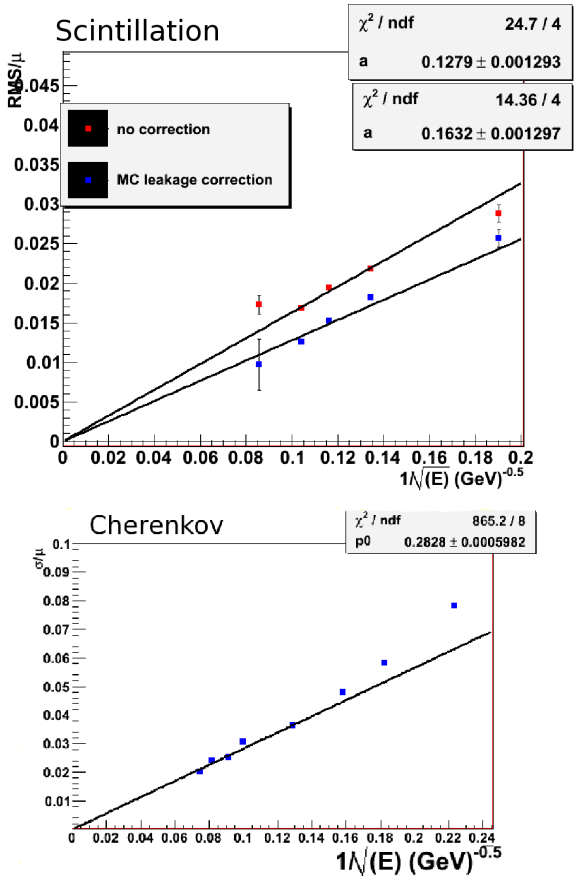


Fig. 11. *Energy resolution as a function of the beam energy. Top: scintillation signals; red not corrected, blue: corrected for longitudinal effects. Bottom: Cherenkov energy resolution; Cherenkov signal is the sum between upstream and downstream signals from the U330 filters.*

The beam energy is plotted on a scale linear in its inverse square root, so that scaling with $E^{-1/2}$ implies the data point to be located on a straight line through the bottom left-hand corner. The experimental data are indeed well described by such a straight line, any energy-independent deviations ("constant terms") are statistically insignificant. The energy dependence of the fractional width of both scintillation and Cherenkov lights is found to scale very well with $E^{-1/2}$. For the scintillation light the measured electromagnetic energy

resolution is:

$$\frac{RMS}{E}(S) = \frac{16.3\%}{\sqrt{E}} \qquad \frac{RMS}{E}(Scorr) = \frac{12.8\%}{\sqrt{E}}$$

while the Cherenkov one is:

$$\frac{\sigma}{E}(C) = \frac{28.3\%}{\sqrt{E}}$$

Due to low-energy events that are out from the tails of the gaussian fit, in the case of scintillation we decided to take, instead of the $\sigma$ from the gaussian fit, the RMS of the histogram for each energy, fixing the bin width. In the case of Cherenkov light we have taken the $\sigma$ from the gaussian fit, but adding contributions both from upstream and downstream PMTs. Given that about 8% of the beam energy is leaking from the end of the matrix, we have then tried to correct this effect for the scintillation signals ($Scorr$). In order to do that, we have simulated the energy loss distribution due to scintillation, for each energy tested. We have then subtracted in quadrature the RMS of the real and the simulated histograms. The result is shown in figure 11 top, blue dots[4].

In figure 12 the response of scintillation and Cherenkov signals as a function of the beam energy is displayed. Response is defined as the average signal per unit of deposited energy:

$$R_S = \frac{< S >}{E} \qquad R_C = \frac{< C >}{E}$$

In the case of full-containment and linear calorimeter, response should be 1; in our case it is around 0.93 because of the longitudinal leakage. Over the measured energy range: 30-150 GeV for S, 20-180 GeV for C, the $PbWO_4$ em calorimeter turned out to be linear to within $\approx$ 1% for scintillation light and 6% for Cherenkov light (red and blue bands in the figure), in fact the response is constant with respect to the beam energy. Widths of the colored bands are indicative for the measurement uncertainties, and show the energy dependent effects of longitudinal leakage and light attenuation in the crystals. In case of Cherenkov light, being photoelectrons less than scintillation ones, at low energies noise effects from the readout system could affect our measurements. More checks about this are ongoing.

November 21, 2011

## V. Conclusion

Preliminary results on 0.3% Mo-doped $PbWO_4$ matrix are very promising in view of its application as an electromagnetic section of an hybrid crystal-fibers Dual Readout calorimeter. Hadron data using this system have still to be taken, once the newdream fiber calorimeter will be built. Some improvements on the electromagnetic performances of the matrix are under study, as the extraction of both Cherenkov and scintillation signal from the same phototube, using time information, exploiting the high rate readout sampling. This solution allows to read crystals only on one side, halving the number of readout channels.

[4]The same correction was not applied to the Cherenkov energy resolution because up to now we have implemented in the MonteCarlo only scintillation processes.

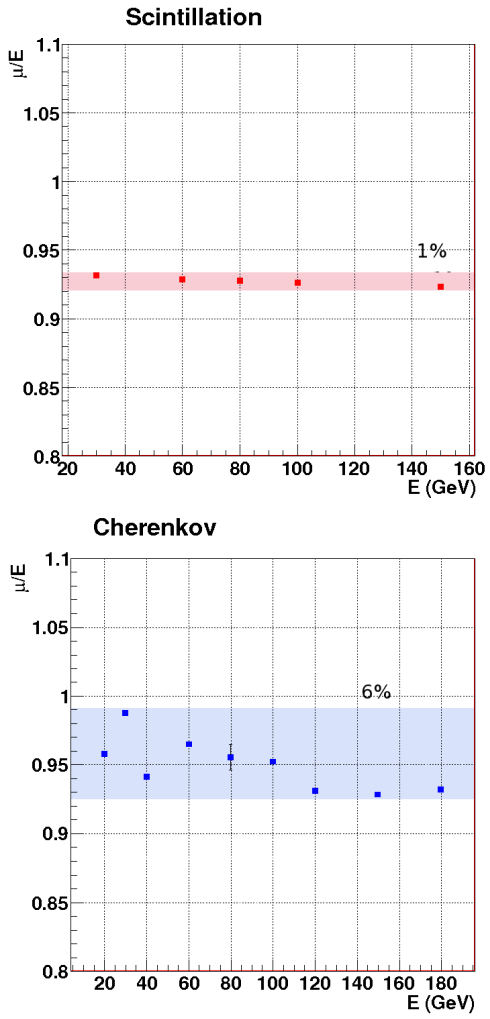


Fig. 12. *Response as a function of the beam energy. Top: scintillation signals, bottom: Cherenkov signals.*

## References


[1] N.Akchurin *et al.*, Nucl. Instr. and Meth. **A536** (2005) 29.
[2] N.Akchurin *et al.*, Nucl. Instr. and Meth. **A537** (2005) 537.
[3] N.Akchurin *et al.*, Nucl. Instr. and Meth. **A582** (2007) 474.
[4] N.Akchurin *et al.*, Nucl. Instr. and Meth. **A595** (2008) 359.
[5] N.Akchurin *et al.*, Nucl. Instr. and Meth. **A640** (2011) 91.
[6] N.Akchurin *et al.*, Nucl. Instr. and Meth. **A**(2008).
[7] N.Akchurin *et al.*, Nucl. Instr. and Meth. **A581** (2007) 643.
[8] N.Akchurin *et al.*, Nucl. Instr. and Meth. **A584** (2008) 273.
[9] R. Wigmans, Calorimetry - Energy Measurement in Particle Physics, International Series of Monographs on Physics, vol. 107, Oxford University Press, Oxford, 2000.
[10] N.Akchurin *et al.*, Nucl. Instr. and Meth. **A399** (1997) 202.
[11] N.Akchurin *et al.*, Nucl. Instr. and Meth. **A638** (2010) 47.
[12] M.V.Korzhik *et al.*, Proc. IEEE Nucl. Sci. Symp., Dresden (2008).
[13] M.Nikl *et al.*, Journal of Applied Physics **104** (2008) 1.
[14] M.Nikl *et al.*, Journal of Applied Physics **91** (2002) 2791.
[15] N.Akchurin *et al.*, Nucl. Instr. and Meth. **A604** (2009) 512.
[16] N.Akchurin *et al.*, Nucl. Instr. and Meth. **A621** (2010) 212.
[17] http://www.caen.it/csite/CaenProd.jsp?idmod=661parent=11